

## A FILM-PORE-SURFACE CONCENTRATION DEPENDENT MODEL FOR ADSORPTION OF DYE ONTO ACTIVATED CARBON

THOMAS S. Y. CHOONG<sup>1\*</sup>, T. G. CHUAH<sup>2</sup>, AZNI IDRIS<sup>3</sup>, Y. L. LAI<sup>4</sup> & S. Y. QUEK<sup>5</sup>

**Abstract.** Adsorption process has been gaining its popularity as an effective alternative for separation processes. Two fundamental properties that determine the adsorption rate are the adsorption equilibrium and the mass transfer limitation. The adsorption isotherm is obtained from batch studies. The mass transfer coefficients of the batch studies need to be extracted by matching the model with the experimental data. For dye adsorption on activated carbon, concentration dependent surface diffusivity is the most important mass transfer parameter and must be included in the study. The pore diffusivity should also be included to improve the accuracy of the simulation. In this work, a mathematical model for adsorption rate was developed based on the film-pore-concentration dependent surface diffusion (FPCDSD) model. The governing partial differential equations (PDEs) were transformed to ordinary differential equations (ODEs) using orthogonal collocation (OC) method. This set of ODEs was then integrated using the numerical algorithm DIVPAG (IMSL library subroutine), which was based on Gear's Method. The FPCDSD model is sufficiently general and can be reduced easily to describe other simpler models for liquid adsorption, such as film-concentration dependent surface diffusion (FCDS) model and film-pore diffusion (FPD) model. The data fitting using the FPD model was unsatisfactory. Both the FPCDSD and the FCDS model were able to fit the experimental data using a single set of mass transfer parameters. However, the  $D_s'$  values for FCDS model were found to be about 30% higher compared to that of the FPCDSD model.

**Keywords:** Adsorption, mass transfer coefficients, activated carbon, dye, diffusion model

**Abstrak.** Proses penjerapan terkenal sebagai satu proses pemisahan alternatif yang berkesan. Dua sifat asas yang menentukan kadar penjerapan ialah keseimbangan penjerapan dan had pemindahan jisim. Garis sesuhu penjerapan diperolehi daripada kajian kelompok. Pekali pemindahan jisim bagi kajian kelompok diperolehi menerusi perbandingan antara model dengan data eksperimen. Bagi penjerapan pewarna pada karbon teraktif, kemeresapan permukaan bersandar kepekatan merupakan parameter pemindahan jisim yang paling penting dan mesti dimasukkan ke dalam kajian. Kemeresapan liang juga mesti dimasukkan demi meningkatkan ketepatan penyelakuan. Dalam kajian ini, satu model matematik kadar penjerapan dihasilkan dengan berdasarkan model kemeresapan permukaan bersandar kepekatan-saput-liang (FPCDSD). Persamaan kebezaan separa (PDEs) menaakluk ditransformasikan menjadi persamaan kebezaan biasa (ODEs) menggunakan kaedah penempatan bersama ortogon (OC). Seterusnya ODEs dikamirkan menggunakan algoritma berangka DIVPAG (subrutin pustaka IMSL) yang berdasarkan

<sup>1,2,3&4</sup> Department of Chemical and Environmental Engineering, Faculty of Engineering, Universiti Putra Malaysia, 43400 Serdang, Selangor, Malaysia.

<sup>5</sup> Department of Food Science, Faculty of Food Science and Biotechnology, Universiti Putra Malaysia, 43400 Serdang, Selangor, Malaysia.

\*Corresponding author

kaedah *Gear*. Model *FPCDSD* adalah begitu umum dan boleh diturunkan bagi menghuraikan model yang lebih mudah, misalnya model kemeresapan permukaan bersandar kepekatan-saput (*FCDS*) dan model kemeresapan saput-liang (*FPD*). Pemadanan data menggunakan model *FPD* adalah tidak memuaskan. Sebaliknya, model *FPCDSD* dan *FCDS* boleh dipadankan dengan data eksperimen menggunakan satu set parameter pemindahan jisim. Walau bagaimanapun, nilai *D* bagi model *FCDS* didapati 30% lebih tinggi daripada model *FPCDSD*.

*Kata kunci:* Penjerapan, pekali pemindahan jisim, karbon teraktif, pewarna, model resapan

## 1.0 INTRODUCTION

Dye and pigments are used in many industries such as textile and pulp mills to colour the products. Most dyes have been reported to be hazardous. They contain appreciable concentration of materials with high biological oxygen demand (BOD) and suspended solids [1]. These coloured compounds impede light penetration in the biological treatment plant. They also increase BOD and cause lack of dissolved oxygen to sustain aquatic life. Dyes are toxic to some microorganisms and may cause direct destruction or inhibition of their catalytic capabilities [2].

Many dyes used in the textile industry are difficult to remove by conventional waste treatment methods since they are stable to light and oxidizing agents, and resistant to aerobic digestion. Removal of dyes by economic techniques is required mainly for developing countries such as Malaysia. Some efforts have already been made in this direction by using activated carbon, rice husks, palm kernel activated carbon, and others.

Adsorption is the most widely used of the physical-chemical treatment processes. It is primarily used for the removal of soluble organic with the aid of activated carbon serving as the adsorbent. Furthermore, adsorption on activated carbon is one of the most effective and dependable technologies currently available for the treatment of drinking water and wastewater contaminated with low concentrations of hazardous compound. For effective design of activated carbon adsorption units, a mathematical model that can describe their separation, and provide information on both the adsorption and desorption of individual pollutants accelerately is required.

Activated carbons are microporous carbonaceous materials and their history could be tracked back to 1600 B.C. when wood chars were used for medicinal purposes in Egypt. Commercially available activated carbons are prepared from carbon-containing source materials such as coal (anthracite or brown coal), lignite, wood, nut shell, petroleum, and sometimes synthetic high polymers.

For adsorption of dyes onto activated carbon, a review of the adsorption literature revealed that the incorporation of the concentration dependent surface diffusivity is essential to the success of a model to describe the adsorption rate of dyes onto adsorbent [3]. Earlier work of concentration dependent surface diffusion models were solved based on the unreacted shrinking core model which assumed a rectangular isotherm. This simplified the model and reduced the computational

time involved. However, since the computer hardware has greatly improved, a full mass transfer model incorporating the appropriate isotherm equilibrium for adsorption could now be solved rather easily. This comprehensive model is able to capture fully the details of the intrapellet transport mechanism in adsorbents.

The objective of this work is to develop a film-pore-concentration dependent surface diffusion (FPCDSD) model for batch adsorption. The model was solved numerically by using the method of lines by first discretising the radial domain using orthogonal collocation method. The ODEs were then solved using standard numerical integration algorithm. The accuracy of the computer program were established by (i) validating the simulation results with the analytical solution provided by Tien [4], and (ii) investigating the effect of interior collocation points. The mass transfer coefficients for a particular dye/adsorbent system can be obtained by matching simulation results with experimental results.

## 2.0 FILM-PORE-CONCENTRATION DEPENDENT SURFACE DIFFUSION MODEL

For a general description of intrapellet mass transfer, it is assumed that both pore and surface diffusion are operative. The concentration dependent surface diffusivity is expressed by using the Higashi-Ito-Oishi (HIO) model to correlate the surface diffusivity,  $D_s$ , directly with the fractional surface coverage factor for the adsorbent,  $\theta$ . Other assumptions of this model are:

- (1) At  $t = 0$ , the concentration of solute is uniform at  $C_{b0}$  throughout the solution and is zero in the adsorbent particle.
- (2) Rapid uptake of solute at particle surface.
- (3) The diffusion direction is radial.
- (4) The system is under constant temperature.

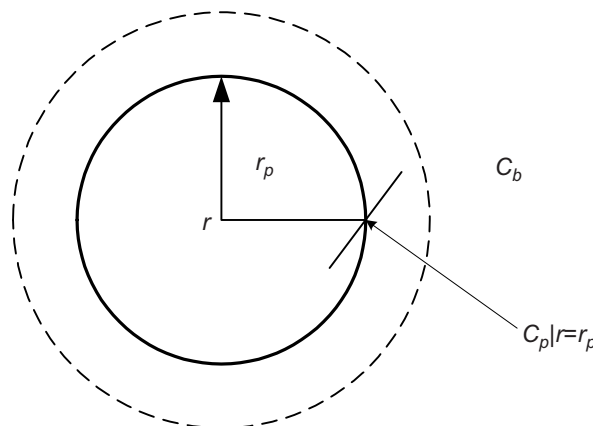


**Figure 1** Schematic representation of an adsorbent particle

Thus, the corresponding macroscopic conservation equation for a spherical adsorbent becomes:

$$\varepsilon_p \frac{\partial C_p}{\partial t} + \rho_p \frac{\partial q}{\partial t} = \frac{1}{r^2} \frac{\partial}{\partial r} \left[ D_p r^2 \frac{\partial C_p}{\partial r} \right] + \frac{\rho_p}{r^2} \frac{\partial}{\partial r} \left[ D_s r^2 \frac{\partial q}{\partial r} \right] \quad (1)$$

where

$$D_s = \frac{D_s'}{1 - \theta} \quad (2)$$

and

$$\theta = \frac{q_{\max}}{q_e} \quad (3)$$

In Equation (3),  $q_{\max}$  indicates the maximum adsorbate adsorbed, and  $q_e$  indicates the amount of the adsorbate adsorbed at equilibrium.

The initial conditions are:

$$C_p(0, r) = 0 \quad (4)$$

and

$$q(0, r) = 0 \quad (5)$$

and the boundary conditions are:

$$\frac{\partial C_p}{\partial r} = 0; \quad r = 0, t > 0 \quad (6)$$

and

$$D_p \frac{\partial C_p}{\partial r} + \rho_p D_s \frac{\partial q}{\partial r} = k_f (C_b - C_p |_{r=R}); \quad r = r_p, t > 0 \quad (7)$$

The relationship between the pore solution phase concentration,  $C_p$ , and the adsorbed phase concentration,  $q$ , is related via the equilibrium isotherm.

Since the actual adsorption step occurs much rapid than the mass-transfer step in physical adsorption, the pore solution concentration and the adsorbed concentration,  $q$ , can be assumed to be in equilibrium:

$$q = f(C_p) \quad (8)$$

with  $f$  representing the isotherm expression. Differentiating Equation (8) yields:

$$dq = f'(C_p) dC_p \quad (9)$$

Substituting Equation (9) into Equation (1) and after some re-arrangement yields:

$$\frac{\partial C_p}{\partial t} = \frac{D_e}{r^2 [\varepsilon_p + \rho_p f'(C_p)]} \frac{\partial}{\partial r} \left[ r^2 \frac{\partial C_p}{\partial r} \right] \quad (10)$$

where  $D_e$  (based on the pore solution concentration) is the effective intrapellet diffusivity, given as:

$$D_e = D_p + f'(C_p) \rho_p D_s \quad (11)$$

Similarly, Equation (7) can be written as:

$$\frac{\partial C_p}{\partial r} = \frac{Bi}{r_p} (C_b - C_p |_{r=r_p}); \quad r = r_p, t > 0 \quad (12)$$

where,  $Bi$  is defined as:

$$Bi = \frac{k_f r_p}{D_e} \quad (13)$$

For the bulk phase, a mass balance yields:

$$-V \frac{dC_b}{dt} = \frac{3M}{4\pi r_p^3 \rho_p} (4\pi r_p^2) \cdot k_f (C_b - C_p |_{r=r_p}) \quad (14)$$

After rearranging Equation (14), it gives:

$$\frac{dC_b}{dt} = -\frac{3M}{r_p \rho_p V} k_f (C_b - C_p |_{r=r_p}) \quad (15)$$

## 2.1 Film-Pore-Surface Diffusion (FPSD) Model

If the surface diffusion is not dependent on concentration, the FPCDSD model is reduced to the FPSD model by setting  $\theta = 0$ .

## 2.2 Film-Concentration Dependent Surface Diffusion (FCDS) Model

If the contribution from the pore diffusion is negligible, the FPCDSD model is reduced to the FCDS model. Equation (11) then becomes:

$$D_e = f'(C_p) \rho_p D_s \quad (16)$$

### 2.3 Film-Surface Diffusion (FSD) Model

If the pore diffusion is negligible, the FPSD model is reduced to the FSD model with  $\theta = 0$  and Equation (16) applies.

### 2.4 Film-Pore Diffusion (FPD) Model

If the surface diffusion is negligible, the FPSD model is reduced to the FPD model with  $\theta = 0$  and Equation (11) is reduced to:

$$D_e = D_p \quad (17)$$

## 3.0 ADSORPTION EQUILIBRIUM

The adsorption isotherm is usually obtained from the equilibrium studies. In order to obtain the isotherm, series of batch studies have to be carried out. The adsorption isotherm relates the concentration of the adsorbate in the bulk phase,  $C_e$  (mg/l) to the concentration of the adsorbate in the solid phase,  $q_e$  (mg/g) at constant temperature. A general form of adsorption isotherm is given by Fritz-Schlünder:

$$q_e = \frac{KC_e^{D_2}}{A + BC_e^{D_1}} \quad (18)$$

where  $K$ ,  $A$ ,  $B$ ,  $D_1$  and  $D_2$  are constants. The two most common adsorption isotherms for liquid adsorption are the Freundlich and the Langmuir isotherms.

### 3.1 Freundlich Isotherm

The Freundlich equation is obtained by setting  $A = 0$  in Equation (18):

$$q_e = K_F C_e^{1/n} \quad (19)$$

The Freundlich isotherm describes equilibrium on a heterogeneous surface where energy of the adsorption is not equivalent for all adsorption sites, thus allowing multi-layer adsorption. The larger the value of adsorption capacity,  $K_F$ , the higher is the adsorption capacity. The more heterogeneous the surface, the closer  $1/n$  is to zero.

### 3.2 Langmuir Isotherm

The Langmuir isotherm can be obtained by setting  $A$ ,  $D_1$ , and  $D_2$  to be unity in Equation (18):

$$q_e = \frac{K_L C_e}{1 + \alpha_L C_e} \quad (20)$$

where  $K_L$  indicates the solute adsorptivity and  $\alpha_L$  is related to the energy of adsorption. The Langmuir isotherm is characterised by a plateau when graphically plotted, which indicates a monolayer adsorption.

#### 4.0 NUMERICAL SIMULATION

The FPCDSD model described above is solved numerically using the method of lines. The governing partial differential equation (PDE) is discretised in the radial direction and is reduced to a set of ordinary differential equation (ODE). Standard numerical integration algorithm is then applied to integrate the ODEs over time.

In this work, the method of orthogonal collocation (OC) is used for spatial discretisation. OC method is chosen as its formulation is convenient to apply and program. Detailed discussion of the OC method could be found in Villadsen and Michelson [5] and Rice and Do [6]. A summary of the method of OC could be found in Choong [7].

A computer program written in FORTRAN 90 was developed for the simulations of the batch adsorbers. Standard algorithms from the IMSL library are employed as external subroutine. The ODE integration algorithm employed the IMSL library subroutine DIVPAG, which is based on a variable order, variable step method implementing backward differentiation formula (Gear's stiff method), and is suitable for stiff system of first order non-linear ODEs. The accuracy of the integration is controlled by the absolute tolerance, TOL, used in the subroutine. The IMSL library subroutine DIVPAG with absolute tolerance,  $TOL = 1 \times 10^{-5}$ , is used for the integration of the system of ODEs.

#### 4.1 Parameters of Modelling

In the batch adsorption simulations, the input parameters are:

- (1) Physical properties of adsorbent: Mass ( $M$ ), density ( $\rho_p$ ), porosity ( $\varepsilon_p$ ), and particle radius ( $r_p$ ).
- (2) Adsorbate specifications: Volume ( $V$ ) and initial sorbate concentration ( $C_{b0}$ ).
- (3) Equilibrium data: Isotherm constants ( $K_L$ ,  $\alpha_L$ ,  $\beta$ ,  $n$ ).
- (4) Mass transfer data: External mass transfer coefficient ( $k_f$ ), pore diffusivity ( $D_p$ ), and surface diffusivity at zero surface coverage ( $D_s'$ ).

The outputs of the program are the dimensionless bulk-phase concentration ( $C_b/C_{b0}$ ) versus time. By matching the simulation and the batch experimental data, the external mass transfer coefficient, pore and surface diffusivities for an adsorbate/adsorbent system can be obtained. The best fit curve is obtained by minimizing the root mean square ( $RMS$ ), given as:

$$RMS = 100 \times \sqrt{\frac{1}{N} \sum_{i=1}^N \left( 1 - \frac{\left( \frac{C_b}{C_{b0}} \right)_{sim,i}}{\left( \frac{C_b}{C_{b0}} \right)_{exp,i}} \right)^2} \quad (21)$$

where  $N$  is the number of experimental points in the concentration decay curve.

An analytical solution to estimate the external mass transfer coefficient had been reported by Furusawa and Smith [8] for liquid batch adsorption and this method was used here to provide initial guess of the external mass transfer coefficient to the computer program.

## 4.2 Establishing the Accuracy of Simulation

Since the mass transfer coefficients were extracted from matching the computer output with the batch experimental data, the accuracy of the simulation needs to be established first. Two steps were taken to ensure the accuracy of simulation. Firstly, the computer program was validated using an analytical solution for finite batch adsorption. Secondly, the effect of the number of collocation points on the accuracy of the simulation was studied.

### 4.2.1 Validation of the Program

The analytical solution provided by Tien [4] for the finite bath was used to validate the result of the simulation. It was assumed that both interphase mass transfer and intrapellet mass transfer were equally significant. For a film-pore-surface diffusion model with linear isotherm, the concentration decay curve for the batch adsorption is given as:

$$\frac{C_b}{C_{b0}} = 1 + \sum_{n=1}^{\infty} \frac{2(1+w)e^{-s_n^2 \tau}}{\left[ 3(1+w) + \frac{s_n^2}{3w + (s_n^2 / Bi)} - \frac{s_n^2}{Bi} \left( 1 - \frac{3Bi}{3wBi + s_n^2} \right) \right] \left[ 1 + \frac{s_n^2}{3wBi} \right]} \quad (22)$$

where  $\tau$  is the dimensionless time defined as:

$$\tau = \frac{t}{r_p^2} \cdot \frac{D_p + \rho_p K D_s}{\varepsilon_p + \rho_p K} \quad (23)$$

where  $K$  is linear isotherm constant, and  $w = \frac{MK}{V}$ .



The eigen values,  $s_n$  are the roots of the following equation:

$$\frac{S_n}{3w} + \left(1 - \frac{s_n^2}{3wBi}\right) (1 - s_n \cdot \cot s_n) = 0 \quad (24)$$

where  $Bi$  is defined by Equation (13).

The  $s_n$  could be conveniently calculated using Goal-seek command in Excel Spreadsheet.

For validation, the simulations were carried out using  $w = 10$ , with Biot numbers of 10 and 100, respectively. The simulation results shown in Figures 2 and 3 have an excellent agreement with the analytical solution, given by Equation (22).

#### 4.2.2 The Effect of Number of Interior Collocation Points on Accuracy of Simulation

The FPCDSD model described earlier was solved numerically using the method of lines (OC method). The accuracy of the simulation increase with the number of interior collocation points. However, as the number of ODEs generated was proportional to the number of interior collocation points, an increase in the number of interior collocation points will result in a longer computational time for solutions. Therefore, a balance must be achieved.

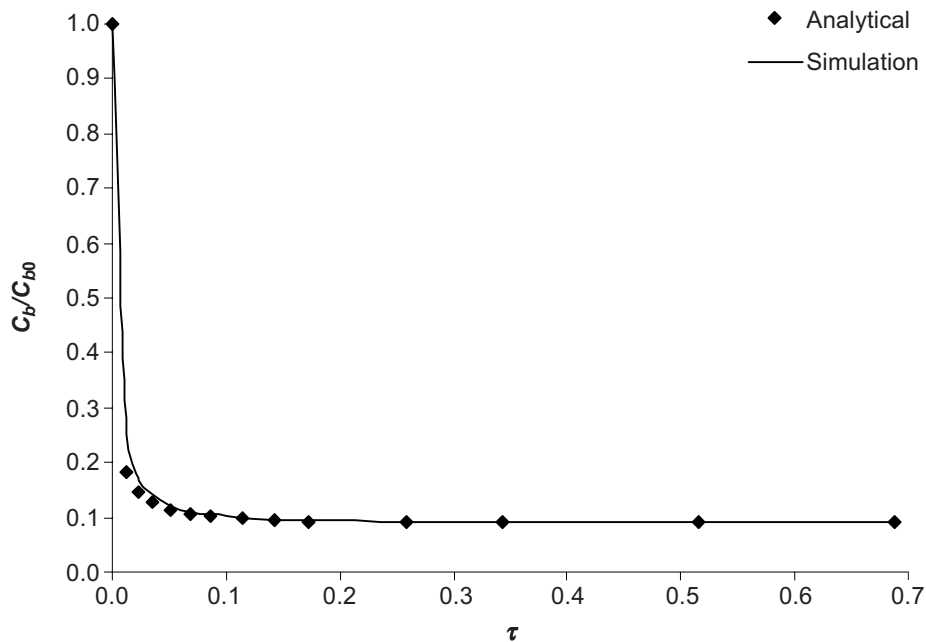


**Figure 2** Dimensionless bulk concentration ( $C_b/C_{b0}$ ) versus dimensionless time,  $\tau$  for  $Bi = 10$  and  $w = 10$  ( $JK = 20$ )

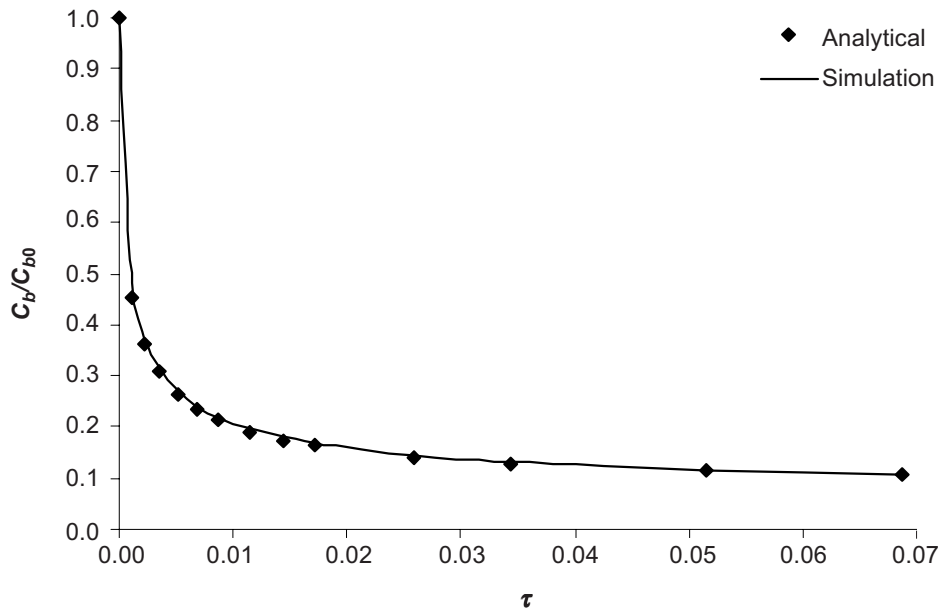


**Figure 3** Dimensionless bulk concentration ( $C_b/C_{b0}$ ) versus dimensionless time,  $\tau$  for  $Bi = 100$  and  $w = 10$  ( $JK = 20$ )

In this work, the effect of the number of interior collocation points on the accuracy of simulation results and the required CPU time were studied. The results are shown in Table 1 and Figure 4. Figure 4 shows that there were little differences in the simulated concentration decay curves after 20 interior collocation points. However, the CPU time was about a factor of 600 for  $JK = 20$  and  $JK = 100$ . Therefore, 20 interior collocation points was considered to provide sufficient accuracy and used in this work for batch adsorption simulation.

**Table 1** Effect of total number of interior collocation points ( $JK$ ) on the CPU time for AR 114/activated carbon system. Simulation conditions are as listed in Tables 2 and 4

$JK$	CPU time (s)
5	$6.25 \times 10^{-2}$
10	$1.25 \times 10^{-1}$
20	$6.09 \times 10^{-1}$
50	$1.28 \times 10^1$
100	$3.85 \times 10^2$

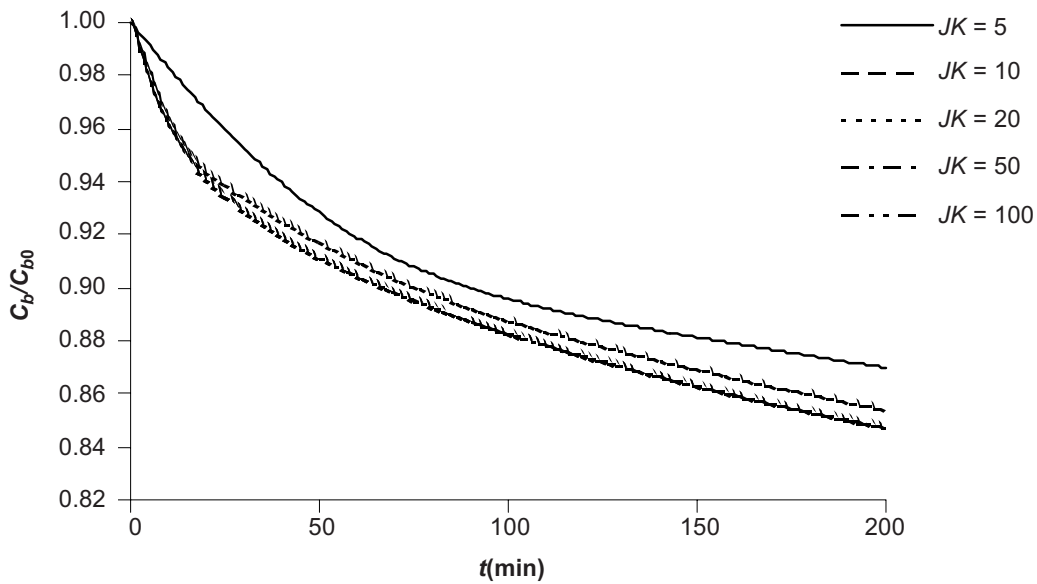


**Figure 4** Dimensionless bulk concentration ( $C_b/C_{b0}$ ) versus time ( $t$ ) for FPCDSD model. (AR114/activated carbon system)

## 5.0 RESULTS AND DISCUSSION

Three representative cases from the adsorption of acid dyes described in the work of Choy *et al.* [9] had been selected to test the applicability of the FPCDSD model in simulating batch adsorption. These are:

- (1) Acid Blue 80 on activated carbon,
- (2) Acid Red 114 on activated carbon, and
- (3) Acid Yellow 117 on activated carbon.

The Langmuir isotherm parameters were taken directly from Choy *et al.* [9]. Apart from the FPCDSD model, two other models, namely the FCDS and the FPD were also used to simulate the batch studies. Figures 5 to 13 show the experimental data and the simulation results for the Acid Blue 80 (AB 80), Acid Red 114 (AR 114), and Acid Yellow 117 (AY 117) for three different models, respectively. The simulation parameters and results are tabulated in Tables 2 to 4.

It is obvious that the film-pore-concentration dependent surface diffusion model has the best fit with the experimental data with the lowest RMS values for all ranges of adsorbent mass under investigation. Results of the RMS for the three models are listed in Table 4. The best fitting is given by the FPCDSD model as indicated in the graph, with the lowest RMS. A single set of mass transfer parameter is able to fit the concentration decay curves of different masses. It was found that the FCDS model

is also able to provide reasonable fitting to the experimental data using one set of mass transfer parameters at higher adsorbent mass. However, the  $D_s'$  values are found to be about 30% higher compared to that of the FPCDSD model. The performances of the FPD model for all three cases were not satisfactory.

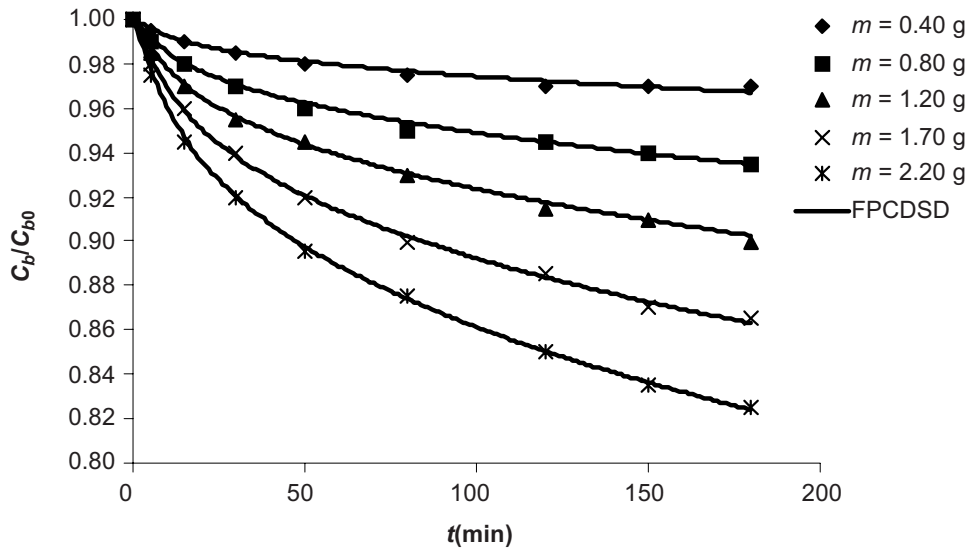


**Figure 5** Dimensionless bulk concentration ( $C_b/C_{b0}$ ) versus time ( $t$ ) for FPCDSD model (AB80/activated carbon system with  $k_f = 4.20 \times 10^{-4} \text{ cm s}^{-1}$ ,  $D_p = 8.80 \times 10^{-8} \text{ cm}^2 \text{ s}^{-1}$ ,  $D_s' = 8.30 \times 10^{-11} \text{ cm}^2 \text{ s}^{-1}$ )

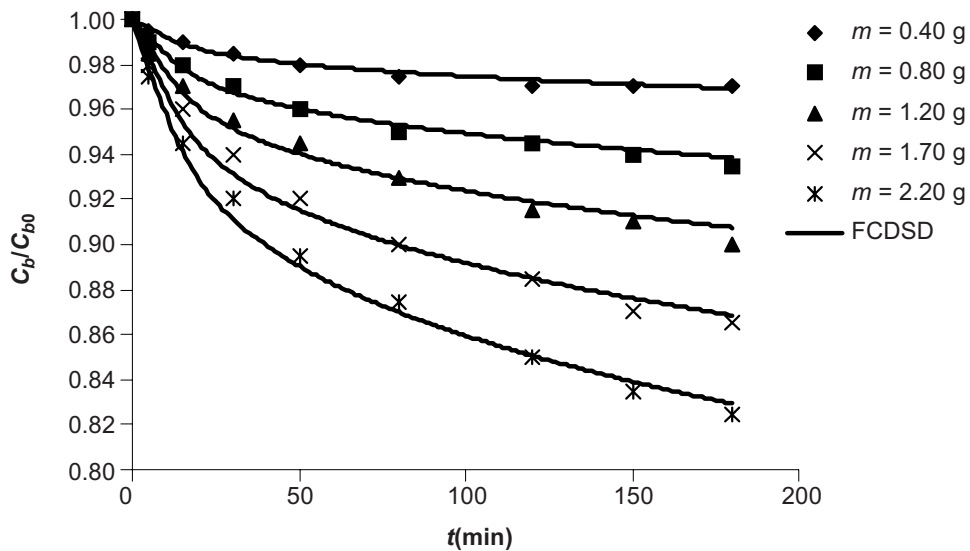


**Figure 6** Dimensionless bulk concentration ( $C_b/C_{b0}$ ) versus time ( $t$ ) for FCDS model. (AB80/activated carbon system) ( $k_f = 4.20 \times 10^{-4} \text{ cm s}^{-1}$ ,  $D_s' = 1.50 \times 10^{-10} \text{ cm}^2 \text{ s}^{-1}$ )

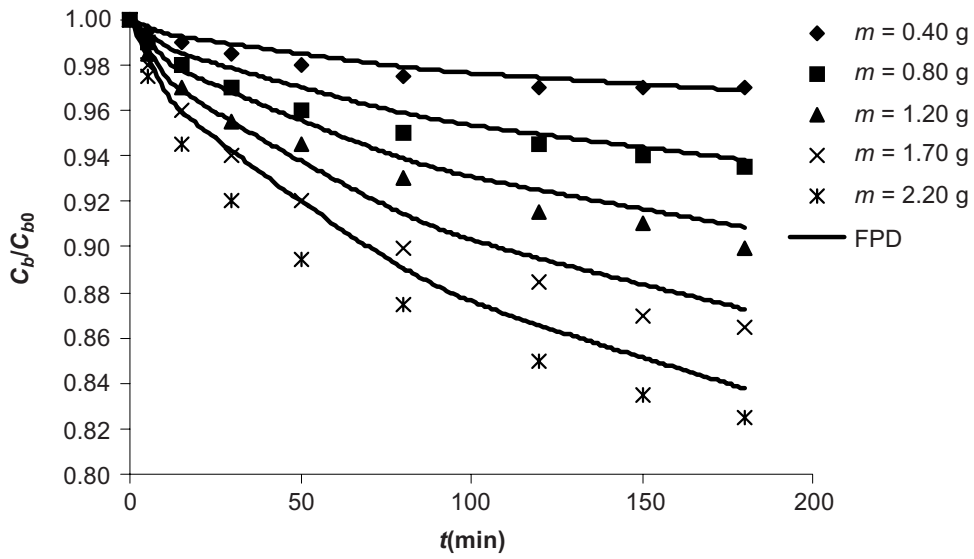


**Figure 7** Dimensionless bulk concentration ( $C_b/C_{b0}$ ) versus time ( $t$ ) for FPD model (AB80/activated carbon system with  $k_f = 4.20 \times 10^{-4} \text{ cm s}^{-1}$ ,  $D_p = 5.92 \times 10^{-8} \text{ cm}^2 \text{ s}^{-1}$ )

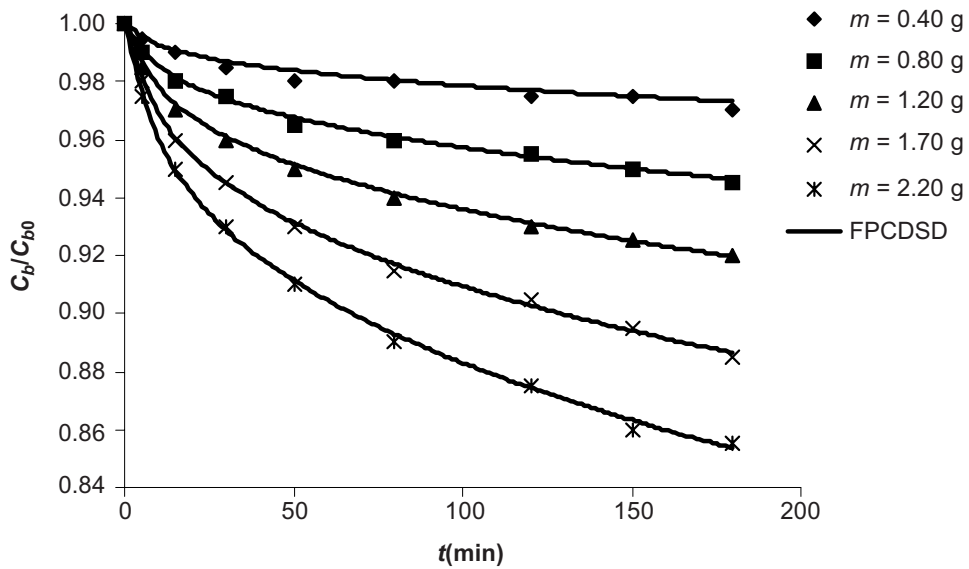


**Figure 8** Dimensionless bulk concentration ( $C_b/C_{b0}$ ) versus time ( $t$ ) for FPCDSD model (AR114/activated carbon system with  $k_f = 4.69 \times 10^{-4} \text{ cm s}^{-1}$ ,  $D_p = 3.38 \times 10^{-8} \text{ cm}^2 \text{ s}^{-1}$ ,  $D_s' = 1.29 \times 10^{-10} \text{ cm}^2 \text{ s}^{-1}$ )

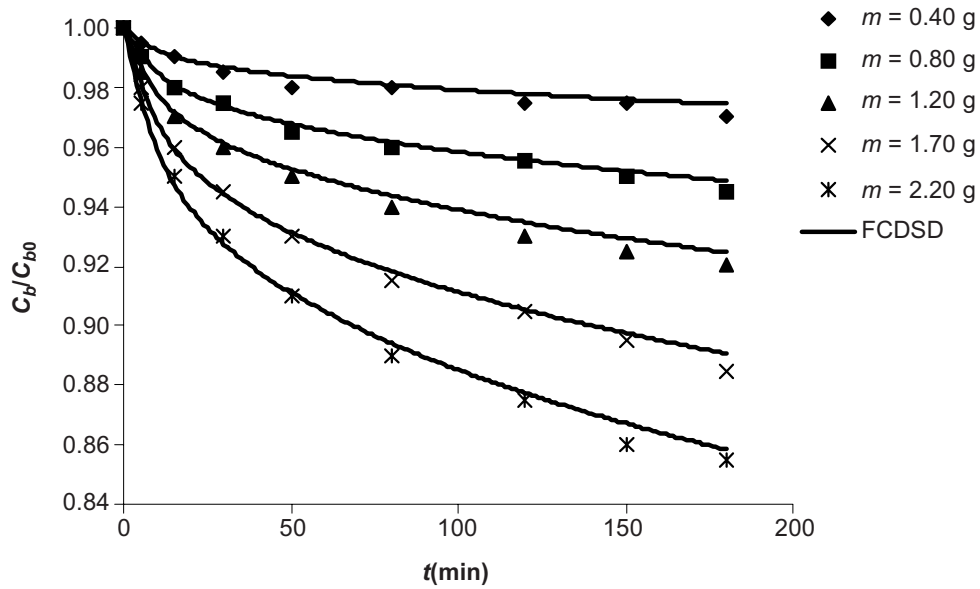


**Figure 9** Dimensionless bulk concentration ( $C_b/C_{b0}$ ) versus time ( $t$ ) for FCDS model (AR114/activated carbon system  $k_f = 4.69 \times 10^{-4} \text{ cm s}^{-1}$ ,  $D_s' = 1.59 \times 10^{-10} \text{ cm}^2 \text{ s}^{-1}$ )

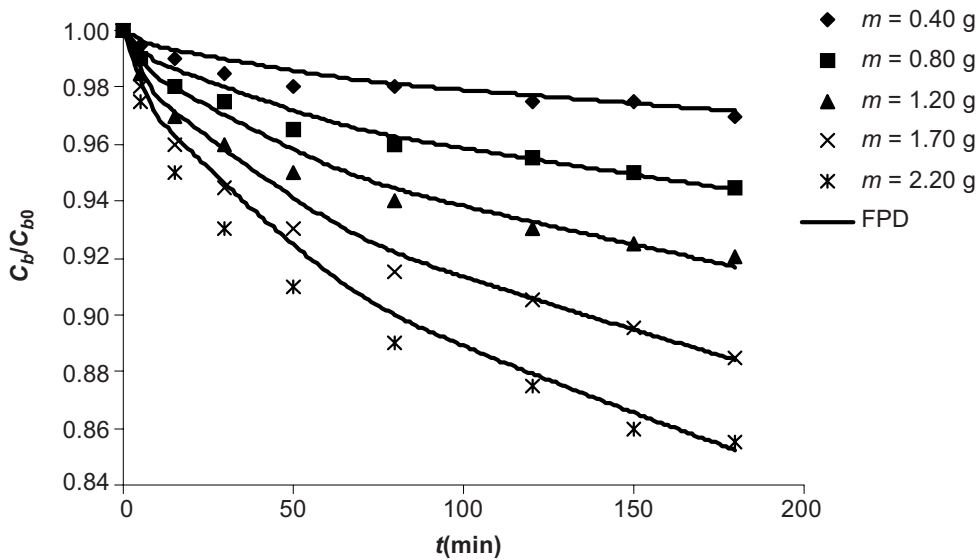


**Figure 10** Dimensionless bulk concentration ( $C_b/C_{b0}$ ) versus time ( $t$ ) for FPD model (AR114/activated carbon system with  $k_f = 4.69 \times 10^{-4} \text{ cm s}^{-1}$ ,  $D_p = 5.78 \times 10^{-8} \text{ cm}^2 \text{ s}^{-1}$ )

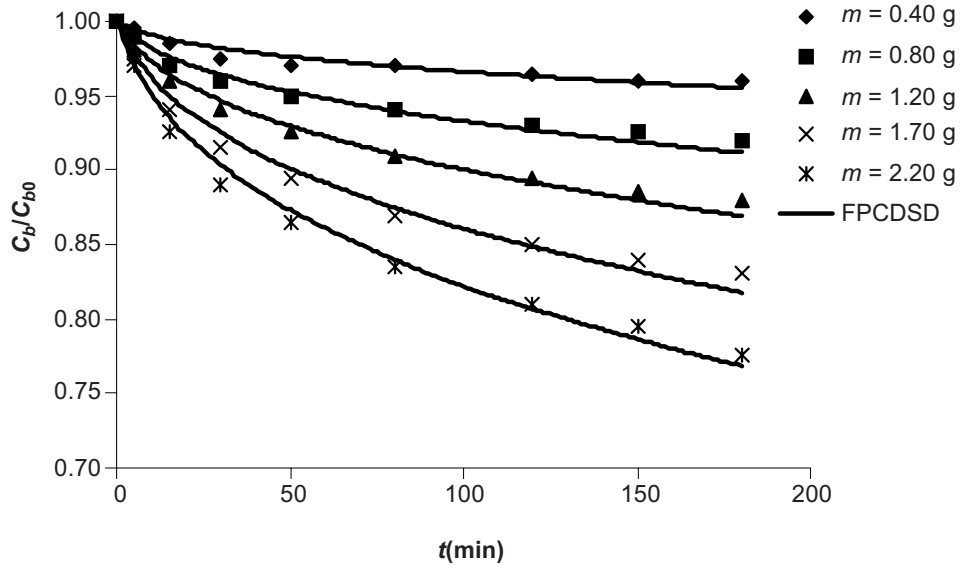


**Figure 11** Dimensionless bulk concentration ( $C_b/C_{b0}$ ) versus time ( $t$ ) for FPCDSD model (AY117/ activated carbon system with  $k_f = 5.84 \times 10^{-4} \text{ cm s}^{-1}$ ,  $D_p = 2.55 \times 10^{-7} \text{ cm}^2 \text{ s}^{-1}$ ,  $D_s = 3.24 \times 10^{-11} \text{ cm}^2 \text{ s}^{-1}$ )

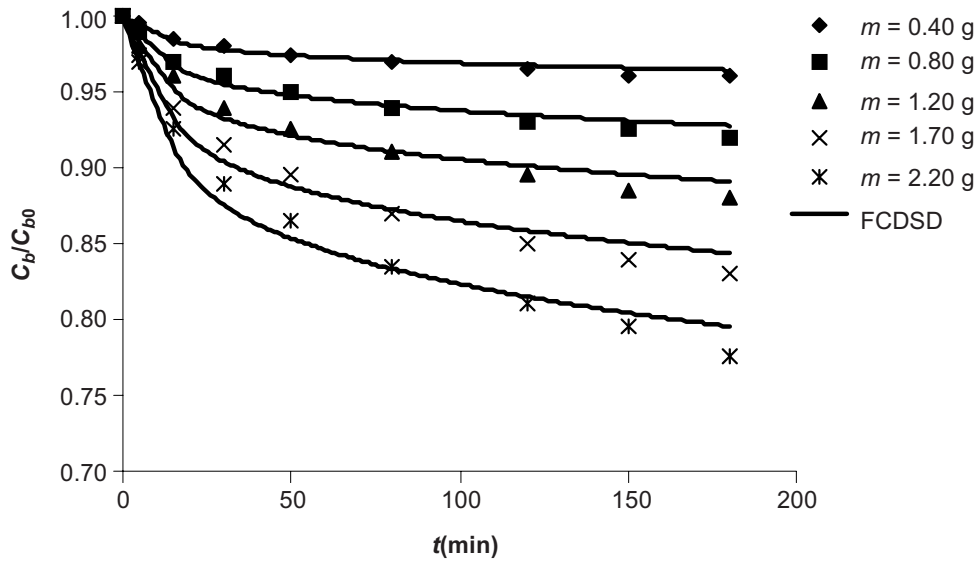


**Figure 12** Dimensionless bulk concentration ( $C_b/C_{b0}$ ) versus time ( $t$ ) for FCDS model (AY117/ activated carbon system with  $k_f = 5.84 \times 10^{-4} \text{ cm s}^{-1}$ ,  $D_s = 1.98 \times 10^{-10} \text{ cm}^2 \text{ s}^{-1}$ )

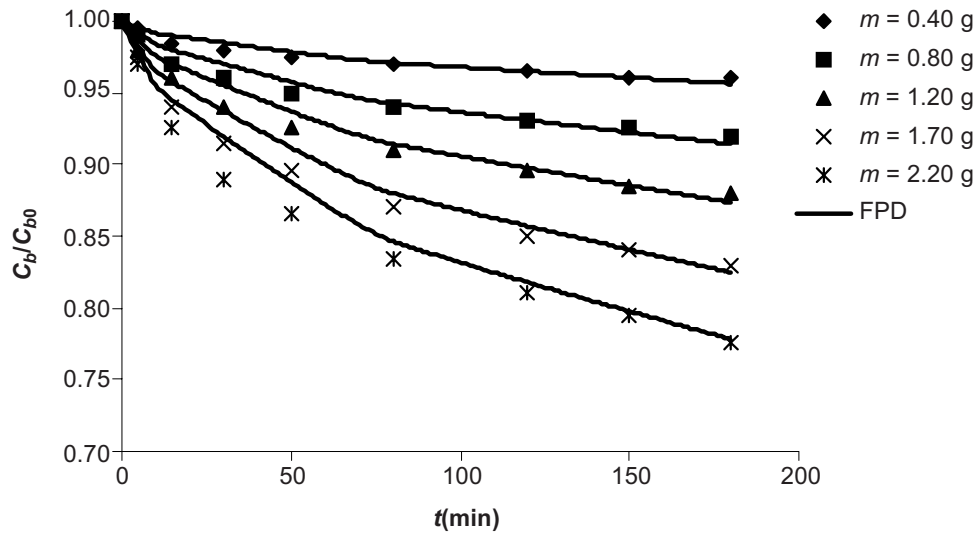


**Figure 13** Dimensionless bulk concentration ( $C_b/C_{b0}$ ) versus time ( $t$ ) for FPD model (AY117/activated carbon system  $k_f = 5.84 \times 10^{-4} \text{ cm s}^{-1}$ ,  $D_p = 9.17 \times 10^{-8} \text{ cm}^2 \text{ s}^{-1}$ )

**Table 2** Values for the parameters of the AB 80/activated carbon, AR 114/activated carbon and AY 117/activated carbon systems under investigation

	AB 80	AR 114	AY 117
Particle density ( $\text{kg} \cdot \text{m}^{-3}$ )	841*	841*	841*
Particle porosity	0.42*	0.42*	0.42*
Particle size ( $\mu\text{m}$ )	605	605	605
Working volume ( $\text{dm}^3$ )	1.7	1.7	1.7
$aL$ ( $\text{dm}^3 \cdot \text{mg}^{-1}$ )	0.5408	0.2689	0.5023
$KL$ ( $\text{dm}^3 \cdot \text{g}^{-1}$ )	60.73	27.84	78.28

\*Estimated from Ruthven [10]



**Table 3** Comparison of three different models for acid dyes/activated carbon system under investigation. The physical properties and working condition are as shown in Table 2

		FPCDSD model	FCDSD model	FPD model
AB 80	$k_f$ (cm·s <sup>-1</sup> )	$4.20 \times 10^{-4}$	$4.20 \times 10^{-4}$	$4.20 \times 10^{-4}$
	$D_p$ (cm <sup>2</sup> ·s <sup>-1</sup> )	$8.80 \times 10^{-8}$	-	$5.92 \times 10^{-8}$
	$D_s'$ (cm <sup>2</sup> ·s <sup>-1</sup> )	$8.30 \times 10^{-11}$	$1.50 \times 10^{-10}$	-
AR 114	$k_f$ (cm·s <sup>-1</sup> )	$4.69 \times 10^{-4}$	$4.69 \times 10^{-4}$	$4.69 \times 10^{-4}$
	$D_p$ (cm <sup>2</sup> ·s <sup>-1</sup> )	$3.38 \times 10^{-8}$	-	$5.78 \times 10^{-8}$
	$D_s'$ (cm <sup>2</sup> ·s <sup>-1</sup> )	$1.29 \times 10^{-10}$	$1.59 \times 10^{-10}$	-
AY 117	$k_f$ (cm·s <sup>-1</sup> )	$5.84 \times 10^{-4}$	$5.84 \times 10^{-4}$	$5.84 \times 10^{-4}$
	$D_p$ (cm <sup>2</sup> ·s <sup>-1</sup> )	$2.55 \times 10^{-7}$	-	$9.17 \times 10^{-8}$
	$D_s'$ (cm <sup>2</sup> ·s <sup>-1</sup> )	$3.24 \times 10^{-11}$	$1.98 \times 10^{-10}$	-

\*Choy *et al.* [9] used the FPCDSD model based on unreacted shrinking core model.

**Table 4** Comparison of RMS values for acid dyes/activated carbon system under different models. The physical properties, working condition, and mass transfer coefficients are as shown in Tables 2 and 3

	Carbon mass (g)	FPCDSD model	FCDSD model	FPD model
		RMS	RMS	RMS
AB 80	0.40	0.1465	0.1413	0.3384
	0.80	0.1681	0.2194	0.6547
	1.20	0.1869	0.4110	0.9377
	1.70	0.2074	0.4904	1.2906
	2.20	0.1814	0.4995	1.8257
AR 114	0.40	0.1968	0.2346	0.3080
	0.80	0.1363	0.1961	0.4034
	1.20	0.1421	0.3397	0.6355
	1.70	0.1567	0.2767	0.8061
	2.20	0.1992	0.3859	1.0582
AY 117	0.40	0.3828	0.2839	0.4008
	0.80	0.4765	0.4476	0.6140
	1.20	0.5875	0.7456	0.8784
	1.70	0.8233	0.9502	1.3391
	2.20	0.8764	1.2835	1.7141

## 6.0 CONCLUSIONS

A three-resistance model based on external mass transfer, pore and concentration dependent surface diffusion was developed in the present work. Simulation results showed that both the FPCDSD and FCDSM models were able to fit the experimental data using a single set of mass transfer parameters. Thus, surface diffusion is the most important mass transfer parameter involved in the adsorption of acid dyes onto activated carbon. However, the  $D_s$  values for FCDSM model were found to be about 30% higher compared to that of the FPCDSD model. This suggests that the inclusion of pore diffusion is essential to obtain accurate values of mass transfer coefficients for dye adsorption onto activated carbon.

## ACKNOWLEDGEMENTS

The authors would like to acknowledge Universiti Putra Malaysia for the financial support.

## NOTATION

$A$	constant	
$a_L$	energy of adsorption	$(\text{dm}^3 \cdot \text{mg}^{-1})$
$B$	constant	
$Bi$	biot number	
$C_0$	initial concentration	$(\text{mg} \cdot \text{l}^{-1})$
$C_b$	bulk concentration	$(\text{mg} \cdot \text{l}^{-1})$
$C_e$	bulk phase concentration	$(\text{mg} \cdot \text{l}^{-1})$
$C_p$	pore solution phase concentration	$(\text{mg} \cdot \text{l}^{-1})$
$D_1, D_2$	constant	
$D_e$	effective diffusivity	$(\text{cm}^2 \cdot \text{s}^{-1})$
$D_p$	pore diffusivity	$(\text{cm}^2 \cdot \text{s}^{-1})$
$D_s$	surface diffusivity	$(\text{cm}^2 \cdot \text{s}^{-1})$
$D_s'$	surface diffusivity at zero surface coverage	$(\text{cm}^2 \cdot \text{s}^{-1})$
$f$	isotherm expression	
$K$	linear adsorption constant	
$K_F$	Freundlich adsorption capacity	
$k_f$	external mass transfer coefficient	$(\text{cm} \cdot \text{s}^{-1})$
$K_L$	Langmurian solute adsorptivity	$(\text{dm}^3 \cdot \text{g}^{-1})$
$M$	adsorbent mass	$(\text{g})$
$n$	surface heterogeneity	
$q$	adsorbed phase concentration	$(\text{mg} \cdot \text{g}^{-1})$
$q_e$	solid phase concentration	$(\text{mg} \cdot \text{g}^{-1})$
$q_{\max}$	solid phase concentration	$(\text{mg} \cdot \text{g}^{-1})$

$r_p$	particle radius	(cm)
$S$	surface area of adsorbent	( $\text{g} \cdot \text{cm}^{-2}$ )
$s_n$	Eigen value	
$t$	time	(s)
$V$	volume of solution	( $\text{cm}^3$ )
$w$	weight factor	

### Greek letters

$\varepsilon_p$	particle porosity	
$\rho_p$	particle density	( $\text{g} \cdot \text{cm}^3$ )
$\theta$	surface coverage defined by Equation (3)	
$\tau$	dimensionless time	

### Abbreviations

BC	Boundary condition
BOD	Biological oxygen demand
FCDS	Film-concentration dependent surface diffusion
FPCDS	Film-pore-concentration dependent surface diffusion
FPD	Film-pore diffusion
HIO	Higashi-Ito-Oishi
IC	Initial condition
OC	Orthogonal collocation
ODE	Ordinary differential equation
PDE	Partial differential equation
RMS	Root mean square

### REFERENCES

- [1] McKay, G. 1984. Two-resistance Mass Transfer Models for the Adsorption of Dyestuffs from Solutions Using Activated Carbon. *J. Chem. Tech. Biotechnol.* 34A: 294-310.
- [2] Asfour, H. M., M. M. Nassar, O. A. Fadali, and M. S. El-Guendi. 1985. Color Removal from Textile Effluents Using Hardwood Saw Dust as an Adsorbent. *J. Chem. Technol. Biotechnol.* 35A: 28-35.
- [3] Wong, T. N. 2003. Adsorption of Dye from Aqueous Solution by Activated Carbon. MSc. Dissertation. Universiti Putra Malaysia, Malaysia.
- [4] Tien, C. 1994. *Adsorption Calculations and Modeling*. Boston: Butterworth-Heinemann.
- [5] Villadsen, J. V., and M. L. Michelson. 1978. *Solution of Differential Equations by Polynomial Approximation*. New Jersey: Prentice-Hill.
- [6] Rice, R. G., and D. D. Do. 1995. *Applied Mathematics and Modelling for Chemical Engineers*. New York: John Wiley & Sons.
- [7] Choong, T. S. Y. 2000. Algorithm Synthesis for Modelling Cyclic Processes: Rapid Pressure Swing Adsorption. Ph.D. Dissertation. The University of Cambridge. United Kingdom.
- [8] Furusawa, T., and J. M. Smith. 1973. Fluid-particle and Intraparticle Mass Transport Rates in Slurries. *Ind. Eng. Chem. Fundam.* 12: 197.

- [9] Choy, K. K. H., J. F. Porter, and G. McKay. 2001. A Film-Pore-Surface Diffusion Model for the Adsorption of Acid Dyes on Activated Carbon. *Adsorption*. 7: 305-317.
- [10] Ruthven, D. M. 1984. *Principles of Adsorption and Adsorption Processes*. New York. John Wiley & Sons.